Electrically driven magnetization of diluted magnetic semiconductors actuated by the Overhauser effect

2010 J. Phys.: Condens. Matter 22 216002

(http://iopscience.iop.org/0953-8984/22/21/216002)

J. Phys.: Condens. Matter **22** (2010) 216002 (7pp) doi:10.1088/0953-8984/22/21/216002

Electrically driven magnetization of diluted magnetic semiconductors actuated by the Overhauser effect

L Siddiqui, A N M Zainuddin and S Datta

School of Electrical and Computer Engineering, Purdue University, West Lafayette, IN 47907, USA

E-mail: lsiddiqu@purdue.edu

Received 26 February 2010, in final form 12 April 2010
Published 30 April 2010
Online at stacks.iop.org/JPhysCM/22/216002

Abstract

It is well known that the Curie temperature, and hence the magnetization, in diluted magnetic semiconductors (DMS) like $Ga_{1-x}Mn_xAs$ can be controlled by changing the equilibrium density of holes in the material. Here, we propose that even with a constant hole density, large changes in the magnetization can be obtained with a relatively small imbalance in the quasi-Fermi levels for up-spin and down-spin electrons. We show, by coupling the mean field theory of diluted magnetic semiconductor ferromagnetism with master equations governing the Mn spin-dynamics, that a mere splitting of the up-spin and down-spin quasi-Fermi levels by 0.1 meV will produce the effect of an external magnetic field as large as 1 T as long as the alternative relaxation paths for Mn spins (i.e. spin–lattice relaxation) can be neglected. The physics is similar to the classic Overhauser effect, also called the dynamic nuclear polarization, with the Mn impurities playing the role of the nucleus. We propose that a lateral spin-valve structure in an anti-parallel configuration with a DMS as the channel can be used to demonstrate this effect, as quasi-Fermi level splitting of such magnitude, inside the channel of similar systems, has already been experimentally demonstrated to produce polarization of paramagnetic impurity spins.

1. Introduction

Electrically driven magnetization of diluted magnetic semiconductors (DMS) has the potential to open up new avenues on the map of magneto-electronics and spintronics [1, 2]. In this regard, electrical manipulation of magnetization has already been demonstrated [3–9] and theoretically proposed [10, 11]. The Curie temperature, in these methods, was controlled by *changing the carrier concentration* (Fermi level) while keeping *the carrier spin-subsystems in an equilibrium among themselves*, that is, keeping the quasi-Fermi levels for up-spin ($\mu_\uparrow$) and down-spin ($\mu_\downarrow$) carriers equal. In contrast, in this work we propose that even with a *constant carrier density*, large changes in the magnetization can be obtained with a relatively *small imbalance in the spin population*, that is, a small difference in $\mu_\uparrow$ and $\mu_\downarrow$. We also propose a structure (figure 1(a)) for demonstrating the effect that is within current experimental capabilities. In essence, our proposed scheme is similar to the optical manipulation of magnetization in [7, 12], where an imbalance in the spin population is attained by using circularly polarized light.

Our proposed effect represents a *non-equilibrium* magnetization resulting from a non-equilibrium bath (the carrier spins) constantly trying to restore equilibrium via spin-flip processes due to exchange interaction with localized spins which get polarized in the process. Indeed the physics is similar to the classic Overhauser effect, also called dynamic nuclear polarization (DNP) [13], with the Mn impurities playing the role of the nucleus. To our knowledge this effect has not been employed to actuate non-equilibrium magnetization by electrical excitation although magnetization by optical excitation via, possibly, the same effect [7, 12] and demagnetization via the opposite effect [14] have been experimentally observed. Our proposed effect involves electrically driven dynamic polarization of *interacting* spins (where the polarization of a particular localized spin is affected by the polarization of the neighboring localized spins) and, hence, would be an extension of a similar effect studied in

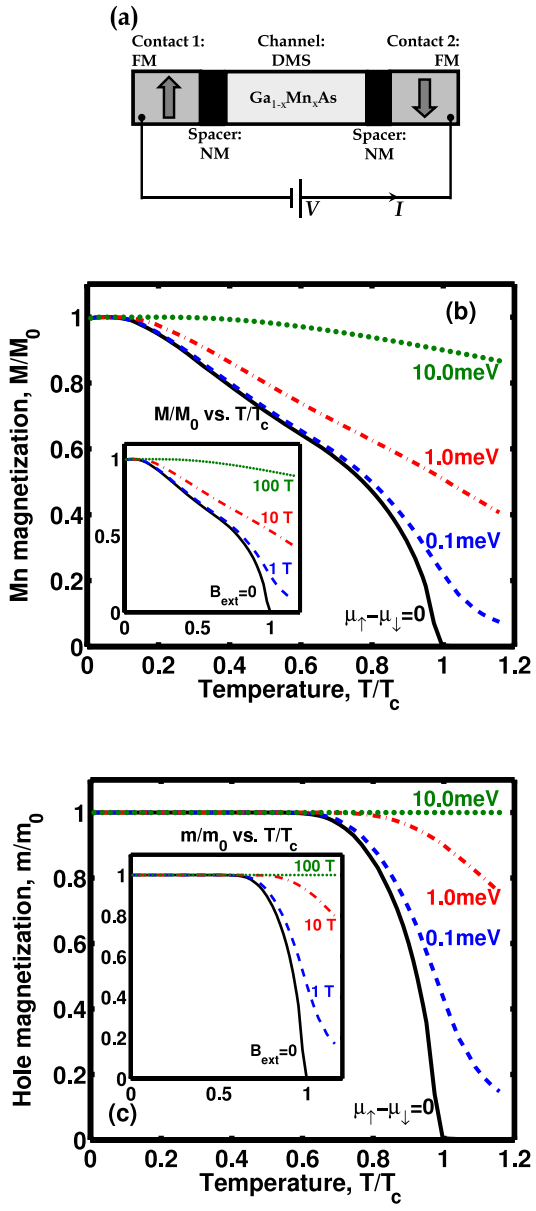

Figure 1. (a) Schematic structure: a dilute magnetic semiconductor (DMS) $Ga_{1-x}Mn_xAs$ connected through nonmagnetic (NM) spacers to two ferromagnetic (FM) contact in an anti-parallel (AP) spin-valve configuration. Under bias V, an electronic current I, injecting spin-polarized carriers (*holes*), flows. (b) Mn magnetization M, scaled by Mn saturation magnetization M_0, versus temperature T, scaled by the Curie temperature T_c, of the channel in (a) for different quasi-Fermi level splitting $\mu_\uparrow - \mu_\downarrow$ ($\mu_{\uparrow(\downarrow)}$ being the channel quasi-Fermi level for up(down)-spin carriers) with external magnetic field $B_{\rm ext} = 0$; *inset*: under different $B_{\rm ext}$ at equilibrium ($\mu_\uparrow - \mu_\downarrow = 0$). (c) Hole magnetization m, scaled by saturation hole magnetization m_0, versus temperature T, scaled by the Curie temperature T_c, of the channel in (a): under the same conditions as in (b); *inset*: under the same conditions as in *inset* of (b). The parameter values for these calculations are: $n_{\rm Mn} \sim 5.0 \times 10^{20}$ cm^{-3}, $n_{\rm h}/n_{\rm Mn} = 0.08$, $m^* = 0.5m_{\rm e}$, $a_0 = 5.65$ Å, and $J = 1$ eV.
(This figure is in colour only in the electronic version)

the context of *non-interacting* spins [15–17]. Due to this effect a splitting of the up-spin and down-spin quasi-Fermi levels in the channel (figure 1(a)) by 0.1 meV can have the same effect as an external magnetic field of 1 T (figure 1(b)). Splitting of this order can be attained by spin-injection into semiconductors [18] and has recently been demonstrated in an n-channel GaAs lateral spin-valve operated with anti-parallel contacts to actuate dynamic polarization of non-interacting spin [19, 20]. A similar p-channel $Ga_{1-x}Mn_xAs$ ($x \sim 0.05$) structure should be suitable for the demonstration of the proposed effect.

2. Model overview

A number of theoretical papers [21–27] have modeled the appearance of ferromagnetic ordering among the Mn ions in $Ga_{1-x}Mn_xAs$, interacting via the itinerant holes, in terms of a mean field description and explain the experimentally observed [28, 29] temperature variation of magnetization in these materials. We adopt exactly the same model as [26] and have modified it to take into account the non-equilibrium aspect by: (i) introducing two different quasi-Fermi levels for up-spin and down-spin holes ($\mu_\uparrow$ and $\mu_\downarrow$ respectively) inside the channel, and (ii) writing a master equation to describe the non-equilibrium dynamics of the Mn spins that was used in [20] to semi-quantitatively explain the experimental observation of Mn spin-dynamics in [19]. In essence, our model is the same as that in [14, 30], which also studies the magnetization dynamics of DMS and uses a more sophisticated valence band description.

With $\mu_\uparrow - \mu_\downarrow = 0$ we get essentially the same results as [26] (solid curves in figures 1(b) and (c)). Under the non-equilibrium situation ($\mu_\uparrow - \mu_\downarrow \neq 0$), according to our model, we expect to see a strong ferromagnetic ordering among the Mn ions (figure 1) for moderate values of $\mu_\uparrow - \mu_\downarrow$ due to reasons that we will discuss later in this paper. A moderate magnitude of $\mu_\uparrow - \mu_\downarrow \sim 0.1$ meV is quite feasible inside the channel of an anti-parallel lateral spin-valve structure [19, 20] and can be understood in terms of a circuit model presented in [19] to explain the experiment therein. We use the same model later in the paper to estimate $\mu_\uparrow - \mu_\downarrow$.

3. Theory

The spontaneous ferromagnetic ordering of the localized Mn spins in a DMS material arises due to the hole mediated exchange interaction between them. In the context of mean field theory of DMS [26], the carriers 'feel' an exchange field due to the polarized Mn spins in addition to any external magnetic field $B_{\rm ext}$, which separates the up-spin band from the down-spin band (figure 2(a)) in energy by

$$\Delta = \Delta_{(\rm ex)} + g_{\rm h}\mu_{\rm B}B_{\rm ext} \qquad \Delta_{(\rm ex)} = Ja_0^3 n_{\rm Mn}\langle S_z^{\rm Mn}\rangle \qquad (1)$$

where a_0 is the lattice constant, $g_{\rm h}$ is the g-factor of the carrier (hole), $\mu_{\rm B}$ is the Bohr magneton, $\Delta_{(\rm ex)}$ is the separation between up-spin band and down-spin band due to exchange field and $\langle S_z^{\rm Mn}\rangle$ is the average z-component of $S = 5/2$ Mn spins:

$$\langle S_z^{\rm Mn}\rangle = \sum_s s\,F_s \qquad (2)$$

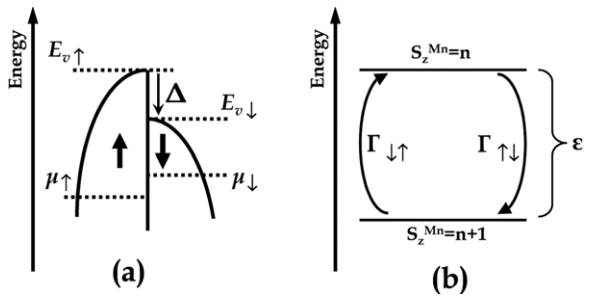

Figure 2. (a) Schematic carrier (hole) bands of the channel in figure 1(a) for different spins: $E_{v\uparrow(\downarrow)}$, $\mu_{\uparrow(\downarrow)}$ and Δ being the valence band edges for up(down)-spin holes, their quasi-Fermi levels and their band splitting respectively. (b) Energy levels and relaxation of Mn spins inside the channel in figure 1(a): $S_z^{\rm Mn}$ denotes the six spin states of the $S = 5/2$ Mn spins, ϵ denotes their energy difference, $\Gamma_{\uparrow\downarrow(\downarrow\uparrow)}$ denotes the rate of transition from lower (higher) z-component state to a higher (lower) z-component state and, $n = -5/2, -3/2, \ldots, 3/2$.

F_s being the probability of a Mn spin being in the $S_z^{\rm Mn} = s$ state ($s = 5/2, 3/2, \ldots, -5/2$).

The carrier band splitting in addition to splitting of quasi-Fermi levels for different carrier spins (figure 2(a)) leads to a non-zero average z-component of hole-spin $\langle S_z^{\rm h}\rangle$ due to unequal carrier concentrations for up-spin ($n_{{\rm h},\uparrow}$) and down-spin ($n_{{\rm h},\downarrow}$), which are given by:

$$\langle S_z^{\rm h}\rangle = \frac{1}{2}\frac{n_{{\rm h},\uparrow} - n_{{\rm h},\downarrow}}{n_{{\rm h},\uparrow} + n_{{\rm h},\downarrow}} \tag{3}$$

$$n_{{\rm h},\uparrow(\downarrow)} = \int {\rm d}E\,(1 - f_{\uparrow(\downarrow)}(E))D_{\uparrow(\downarrow)}(E) \tag{4}$$

where $f_{\uparrow(\downarrow)}(E)$ is the Fermi function with Fermi level $\mu_{\uparrow(\downarrow)}$ and temperature T: $f_{\uparrow(\downarrow)}(E) = [1 + \exp\{(E - \mu_{\uparrow(\downarrow)})/k_{\rm B}T\}]^{-1}$, and $D_{\uparrow(\downarrow)}$ is the three-dimensional density of states for up(down)-spin carriers calculated assuming a parabolic band with an effective mass of m^* and a band-edge at $E_{v\uparrow(\downarrow)}$ (figure 2(a)). $E_{v\uparrow}$, $E_{v\downarrow}$ and Δ are related by $E_{v\downarrow} - E_{v\uparrow} = \Delta$ and the charge neutrality condition: $n_{\rm h} = n_{{\rm h},\uparrow} + n_{{\rm h},\downarrow}$.

The Mn spins on the other hand feel an exchange field due to the spin-polarized carriers in addition to any external magnetic field, which leads to energy level splitting (figure 2(b)),

$$\begin{aligned} \epsilon &= \epsilon_{\rm (ex)} + g_{\rm Mn}\mu_{\rm B}B_{\rm ext} \\ \epsilon_{\rm (ex)} &= Ja_0^3 n_{\rm h}\langle S_z^{\rm h}\rangle \end{aligned} \tag{5}$$

(a new variable $\epsilon_{\rm (ex)}$ appears in the above equation) where $g_{\rm Mn}$ is the g-factor of Mn spins and $\epsilon_{\rm (ex)}$ is the splitting of Mn spin levels due to the exchange field.

Up to this point, all the equations and quantities, except different quasi-Fermi levels $\mu_\uparrow$ and $\mu_\downarrow$, are essentially the same as [26] and take into account the non-equilibrium effects of Mn spin-polarization on the holes. To consider the non-equilibrium effects of the holes on the Mn spins and the resulting non-equilibrium dynamics, we solve the dynamic rate equation, which was also used in [20, 30], for the occupation probabilities F_s:

$$\frac{\rm d}{{\rm d}t}\begin{bmatrix} F_{-5/2} \\ F_{-3/2} \\ F_{-1/2} \\ F_{+1/2} \\ F_{+3/2} \\ F_{+5/2} \end{bmatrix} = \mathbf{\Gamma}\begin{bmatrix} F_{-5/2} \\ F_{-3/2} \\ F_{-1/2} \\ F_{+1/2} \\ F_{+3/2} \\ F_{+5/2} \end{bmatrix} \tag{6}$$

at steady state (by setting ${\rm d}F_s/{\rm d}t = 0$) under the normalization constraint: $\sum_s F_s = 1$ where,

$$\mathbf{\Gamma} = \begin{bmatrix} -\Gamma_{\uparrow\downarrow} & \Gamma_{\downarrow\uparrow} & 0 & 0 & 0 & 0 \\ \Gamma_{\uparrow\downarrow} & -(\Gamma_{\uparrow\downarrow} + \Gamma_{\downarrow\uparrow}) & \Gamma_{\downarrow\uparrow} & 0 & 0 & 0 \\ 0 & \Gamma_{\uparrow\downarrow} & -(\Gamma_{\uparrow\downarrow} + \Gamma_{\downarrow\uparrow}) & \Gamma_{\downarrow\uparrow} & 0 & 0 \\ 0 & 0 & \Gamma_{\uparrow\downarrow} & -(\Gamma_{\uparrow\downarrow} + \Gamma_{\downarrow\uparrow}) & \Gamma_{\downarrow\uparrow} & 0 \\ 0 & 0 & 0 & \Gamma_{\uparrow\downarrow} & -(\Gamma_{\uparrow\downarrow} + \Gamma_{\downarrow\uparrow}) & \Gamma_{\downarrow\uparrow} \\ 0 & 0 & 0 & 0 & \Gamma_{\uparrow\downarrow} & -\Gamma_{\downarrow\uparrow} \end{bmatrix} \tag{7}$$

$\Gamma_{\uparrow\downarrow}$ and $\Gamma_{\downarrow\uparrow}$ (figure 2(b)), as valence band holes surrounding the Mn spins act as their spin-bath and also as Mn spins have negligible spin–lattice relaxation rate in comparison [14], are given by:

$$\Gamma_{\uparrow\downarrow} = \frac{2\pi}{h}J^2\int {\rm d}E\,D_\downarrow(E+\epsilon)(1 - f_\downarrow(E+\epsilon))D_\uparrow(E)f_\uparrow(E) \tag{8a}$$

$$\Gamma_{\downarrow\uparrow} = \frac{2\pi}{h}J^2\int {\rm d}E\,D_\uparrow(E)(1 - f_\uparrow(E))D_\downarrow(E+\epsilon)f_\downarrow(E+\epsilon). \tag{8b}$$

4. Results: non-equilibrium magnetization

The equations (3), (5), (6), (2) and (1), are solved sequentially and self-consistently (figure 3) to calculate the Mn spin polarization and hole polarization in figures 1(b) and (c) respectively. Magnetization of the Mn and holes inside channel material ($Ga_{1-x}Mn_xAs$) is then calculated from: $M = 2M_0\langle S_z^{\rm Mn}\rangle/5$ and $m = 2m_0\langle S_z^{\rm h}\rangle$ respectively, where the corresponding saturation magnetizations, $M_0 = 5g_{\rm Mn}\mu_{\rm B}n_{\rm Mn}/2$ and $m_0 = g_{\rm h}\mu_{\rm B}n_{\rm h}/2$. The iterative loop in figure 3 embodies a positive feedback loop that gives rise to equilibrium magnetization below the Curie temperature in such materials. Such positive feedback in combination with the Overhauser effect (figure 3) is what gives rise to non-equilibrium magnetization even above the Curie temperature. The results of the calculations, shown in figures 1(b) and (c), use realistic parameter values [26] and give equilibrium magnetization characteristics (calculated by setting $\mu_\uparrow - \mu_\downarrow = 0$) similar to experimental observations [28, 29]. Two sets of calculations were performed: (1) calculations for different values of $\mu_\uparrow - \mu_\downarrow$ by setting $B_{\rm ext} = 0$, whose results are shown in the main plots of figures 1(b) and (c), and (2) calculations for

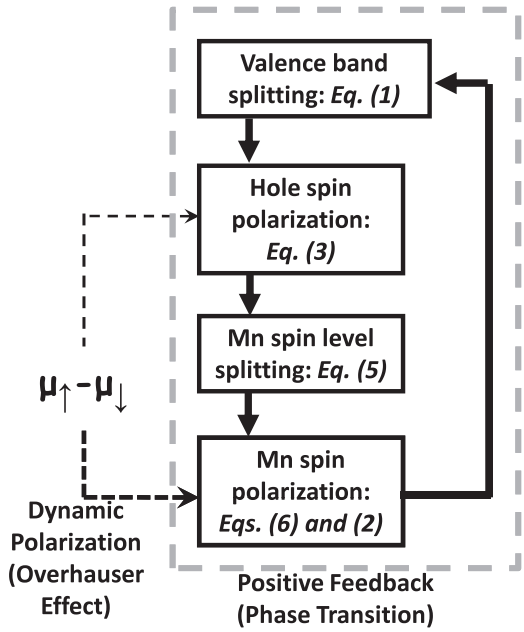

Figure 3. Non-equilibrium magnetization arises from an interplay of dynamic spin-polarization (Overhauser effect) that is driven by the quasi-Fermi level splitting $\mu_\uparrow - \mu_\downarrow$ between up-spin and down-spin holes and a positive feedback that is responsible for equilibrium magnetization below the Curie temperature.

different values of $B_{\rm ext}$ by setting $\mu_\uparrow - \mu_\downarrow = 0$ (equilibrium), whose results are shown in the inset plots of figures 1(b) and (c). By comparing the main plots in figures 1(b) and (c) with their corresponding inset plots, we observe that the values of $\mu_\uparrow - \mu_\downarrow$ corresponding to the curves in the main plots maintain a proportionality relation with the values of $B_{\rm ext}$ corresponding to the similar curves in the corresponding inset plots (0.1 meV:1.0 meV:10.0 meV = 1 T:10 T:100 T). Such a proportionality relation is, by no means, a coincidence and is maintained in the calculations done with different values of J, $n_{\rm Mn}$, and $n_{\rm h}$ (results not shown in this paper). Although the Curie temperature, the saturation magnetization and the shapes of the magnetization versus temperature curves are different for different values of J, $n_{\rm Mn}$, and $n_{\rm h}$ due to the dependence of the exchange field on these parameters (equations (1) and (5)) the strength of the effect remains the same, i.e. the magnetizations for a quasi-Fermi level splitting of 0.1 meV without any external magnetic field, when alternative Mn spin relaxation paths can be neglected, is equal to the magnetizations for an external magnetic field of 1 T at equilibrium. As a result, changing J, $n_{\rm Mn}$, and $n_{\rm h}$ by changing the doping, changing the Mn mole fraction, introducing disorder [31] or by using a different DMS material (that has itinerant carrier mediated exchange interaction of localized spins) will not play any significant role as far as the strength of the effect is concerned, for reasons to be discussed in the next section.

5. Discussion

The results in figures 1(b) and (c) can be anticipated if the effect of $\mu_\uparrow - \mu_\downarrow$ is considered as an effective external magnetic field as far as the hole spin-polarization and Mn spin-polarization are concerned. We can show that the functional dependence of $\langle S_z^{\rm h}\rangle$ on Δ and $\mu_\uparrow - \mu_\downarrow$ obeys the following relation (see appendix A):

$$\langle S_z^{\rm h}\rangle(\Delta, \mu_\uparrow - \mu_\downarrow) = \langle S_z^{\rm h}\rangle(\Delta + \mu_\uparrow - \mu_\downarrow, 0). \qquad (9)$$

The first term is the hole spin-polarization for a valence band splitting of Δ and a non-zero quasi-Fermi level splitting $\mu_\uparrow - \mu_\downarrow$, while the second term corresponds to the hole spin-polarization for an additional valence band splitting of $\mu_\uparrow - \mu_\downarrow$ over the original value Δ and a zero quasi-Fermi level splitting (equilibrium). At this point, one can observe that the results in the main plot (i.e. for $B_{\rm ext} = 0$) and the inset plot (i.e. for $\mu_\uparrow - \mu_\downarrow = 0$) of figure 1(c) (i.e. hole spin-polarization) correspond to $\langle S_z^{\rm h}\rangle(\Delta_{\rm (ex)}, \mu_\uparrow - \mu_\downarrow)$ i.e. $\langle S_z^{\rm h}\rangle(\Delta_{\rm (ex)} + \mu_\uparrow - \mu_\downarrow, 0)$ (equation (9)) and $\langle S_z^{\rm h}\rangle(\Delta_{\rm (ex)} + g_{\rm h}\mu_{\rm B}B_{\rm ext}, 0)$ respectively. The mathematical equivalence of the last two expressions suggests that, as far as hole spin-polarization is concerned, $\mu_\uparrow - \mu_\downarrow$ has the equivalent effect of an effective external magnetic field of $B_{\rm ext}^{\rm h} = (\mu_\uparrow - \mu_\downarrow)/(g_{\rm h}\mu_{\rm B})$. On the other hand, for Mn spins it can also be shown that the functional dependence of $\langle S_z^{\rm Mn}\rangle$ on ϵ and $\mu_\uparrow - \mu_\downarrow$ obeys the following relation (see appendix B):

$$\langle S_z^{\rm Mn}\rangle(\epsilon, \mu_\uparrow - \mu_\downarrow) = \langle S_z^{\rm Mn}\rangle(\epsilon + \mu_\uparrow - \mu_\downarrow, 0). \qquad (10)$$

In this case, the first term is the Mn spin-polarization for an energy level splitting of ϵ and a non-zero quasi-Fermi level splitting of $\mu_\uparrow - \mu_\downarrow$, while the second term corresponds to the Mn spin-polarization for an additional energy level splitting of $\mu_\uparrow - \mu_\downarrow$ over the original value ϵ and a zero quasi-Fermi level splitting (equilibrium). At this point, one can observe that the results in the main plot (i.e. for $B_{\rm ext} = 0$) and the inset plot (i.e. for $\mu_\uparrow - \mu_\downarrow = 0$) of figure 1(b) (i.e. Mn spin-polarization) correspond to $\langle S_z^{\rm Mn}\rangle(\epsilon_{\rm (ex)}, \mu_\uparrow - \mu_\downarrow)$ i.e. $\langle S_z^{\rm Mn}\rangle(\epsilon_{\rm (ex)} + \mu_\uparrow - \mu_\downarrow, 0)$ (equation (10)) and $\langle S_z^{\rm Mn}\rangle(\epsilon_{\rm (ex)} + g_{\rm h}\mu_{\rm B}B_{\rm ext}, 0)$ respectively. The mathematical equivalence of the last two expressions shows that, as far as Mn spin-polarization is concerned, $\mu_\uparrow - \mu_\downarrow$ has the equivalent effect as an effective external magnetic field of $B_{\rm ext}^{\rm Mn} = (\mu_\uparrow - \mu_\downarrow)/(g_{\rm Mn}\mu_{\rm B})$ acting on the Mn spins at equilibrium. For $g_{\rm h} \sim g_{\rm Mn} \sim 2$ the equivalent external magnetic fields for hole spins and Mn spins ($B_{\rm ext}^{\rm h}$ and $B_{\rm ext}^{\rm Mn}$), that are mentioned above, would be equal and be given by

$$B_{\rm ext}^{\rm eff} \approx \frac{\mu_\uparrow - \mu_\downarrow}{2\mu_{\rm B}}. \qquad (11)$$

Herein lies the strength of the effect: a mere difference of 0.1 meV between $\mu_\uparrow$ and $\mu_\downarrow$ is strong enough to produce the effect corresponding to that of an external magnetic field as large as 1 T. One can notice that the arguments presented above do not depend on J, $n_{\rm Mn}$ or $n_{\rm h}$ and require that the alternative relaxation paths for the Mn spins can be neglected (which entered through the neglect of spin–lattice relaxation rate while writing down the equations (8) and was subsequently used in the derivation of equation (10)). As a result, the strength of the effect (equation (11)) is insensitive to a change in J, $n_{\rm Mn}$, and $n_{\rm h}$, and, hence, is relatively insensitive to our choice of mean field (equations (1) and (5)), as long as the

alternative relaxation paths for the Mn spins can be neglected. Since (1) our central result (equation (11)), originating from non-equilibrium magnetization dynamics, is relatively insensitive to our choice of mean field (equations (1) and (5)), (2) equations (1) and (5) describe the equilibrium temperature dependence of magnetization, at least, qualitatively [26], and (3) a model [30], which essentially uses our choice of mean field, has been used to successfully explain recent experiments [14] on non-equilibrium magnetization dynamics, we feel justified in leaving it to future work to assess the need for improving equations (1) and (5).

Experimental realization of quasi-Fermi level splitting, similar to the values mentioned above, has already been demonstrated to drive dynamic polarization of non-interacting spins [19, 20] with a structure similar to the one shown in figure 1(a). One can quite legitimately envision that with further improvement of the spin-injection process in terms of contact polarization P_c and contact conductance and, hence, the parallel terminal conductance $G_\parallel$, one can achieve even higher $\mu_\uparrow - \mu_\downarrow$, leading to a higher degree of ferromagnetic ordering that would otherwise require immensely large magnetic fields (figure 1). The material property of the DMS that acts against attaining quasi-Fermi level splitting between up-spin and down-spin holes is the spin lifetime of the valence band holes τ_{so} independent of Mn that give rise to the spin-flip conductance g_{so}. The effect of all these ingredients of a spin-valve structure on $\mu_\uparrow - \mu_\downarrow$ can be concisely pictured in terms of the circuit model in figure 4(a), which we have adopted from [19] and is valid for a channel length in figure 1(a) that is smaller than the spin-diffusion length. Since the spin-diffusion length of magnetic semiconductors has not, to the best of our knowledge, been reported in the literature, we are unable to conclusively comment, as far as the channel length is concerned, on the scope of the analysis to follow, and will limit our analysis to the thinnest possible (2D) channel having a thickness of atomic dimensions in the transport direction. Nevertheless, it will touch upon some key ingredients that affect $\mu_\uparrow - \mu_\downarrow$. Moreover, the derivation of equations (9) and (10) do not rely on the shape of the density of states as long as the density of states for both up-spin and down-spin carriers have the same energy dependence (so that one can write: $D_\uparrow(E) = D_\downarrow(E+\Delta)$). As a result, as far as the strength of the effect is concerned, whether the channel is 2D or 3D does not play any significant role.

Upon simplification of that circuit model, as shown in figure 4(b), we get: $\mu_\uparrow - \mu_\downarrow = qVP_c(1 + \frac{g_{so}}{G_\parallel})^{-1}$, where V is the applied bias and q is the electronic charge. We estimate $g_{so} \sim 10^{10}\ \Omega^{-1}\ \mathrm{m}^{-2}$ for $Ga_{1-x}Mn_xAs$ from the relation $g_{so} = \frac{q^2}{h} D \frac{\hbar}{\tau_{so}}$, using $\tau_{so} = 1$ ps (spin life-time of GaAs valence band holes [32]) and a 2D density of states value $D \sim 10^{37}\ \mathrm{J}^{-1}\ \mathrm{m}^{-2}$ (estimated using the valence band effective mass used in figure 1(b), which is of the same order of magnitude as the number calculated from the 3D density of states for a thickness of atomic dimensions (∼1 nm)). For such a value of g_{so}, if we use the terminal conductance and contact polarization values of [19, 20] ($G_\parallel \sim 10^7\ \Omega^{-1}\ \mathrm{m}^{-2}$, $P_c \sim 0.5$), we estimate $\mu_\uparrow - \mu_\downarrow \sim 1$ meV for an applied voltage of $V = 1$ V. However, for $\tau_{so} = 10$ fs (the value used in [14]) one would have to increase $G_\parallel$ to $\sim 10^9\ \Omega^{-1}\ \mathrm{m}^{-2}$ (similar to the values in [33]) to get the same effect.

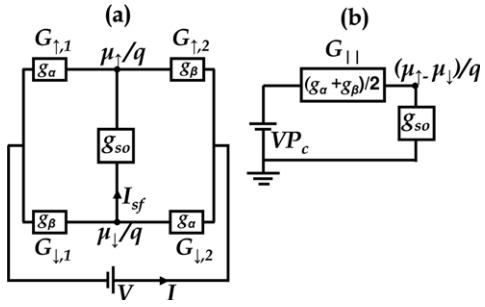

Figure 4. (a) Circuit model of the structure in figure 1(a) (adopted from [19]): g_{so}, $G_{\uparrow(\downarrow),1}$, $G_{\uparrow(\downarrow),2}$, g_α and, g_β are the carrier spin-flip conductance independent of Mn spins, contact 1 conductance for up(down)-spin, contact 2 conductance for up(down)-spin, majority spin conductance and, minority spin conductance respectively. (b) Simplified circuit diagram of the model circuit in (a): $G_\parallel$ and $P_c = (g_\alpha - g_\beta)/(g_\alpha + g_\beta)$ are the terminal conductance for the parallel (P) configuration and the contact polarization respectively.

6. Summary

In summary, we have proposed a novel mechanism for attaining and controlling ferromagnetic ordering in DMS materials. We argue that the non-equilibrium accumulation of carrier spins drives the spin alignment of magnetic impurities in DMS via the exchange interaction which is responsible for the origin of the ferromagnetism in such materials in the first place. We find the effect to be quite strong when we consider that such a degree of ferromagnetic ordering would otherwise have to be attained by applying a very large magnetic field and, also, that this strength is insensitive to a change in several crucial parameters (magnetically active Mn concentration, hole concentration, and strength of exchange interaction between Mn spins and valence band holes) that describe the equilibrium ferromagnetism of such systems. We believe that, with the existing experimental sophistication achieved over the years, our proposed scheme could be realized in the near future and will usher in a new paradigm in the experimental investigation of ferromagnetic phase transition and also in applications benefitting from the strong control of magnetism, for example magnetocaloric applications [34].

Acknowledgment

This work is supported by the Office of Naval Research under Grant No. N00014-06-1-0025.

Appendix A. Derivation of equation (9)

Starting from equations (3) and (4) we get

$$\langle S_z^h\rangle(\Delta, \mu_\uparrow - \mu_\downarrow) = \frac{1}{2n_h}\left[\int \mathrm{d}E\,\{D_\uparrow(E) - D_\downarrow(E)\} - \int \mathrm{d}E\,\{f_\uparrow(E)D_\uparrow(E) - f_\downarrow(E)D_\downarrow(E)\}\right] \quad \text{(A.1)}$$

where n_h was assumed to remain constant (varying with neither Δ nor $\mu_\uparrow - \mu_\downarrow$) on the ground of charge neutrality. Now, for a given valence band splitting Δ and a given quasi-Fermi level splitting $\delta\mu \equiv \mu_\uparrow - \mu_\downarrow$ (figure 2) we can write

$$D_\uparrow(E) = D_\downarrow(E + \Delta) \equiv D(E) \tag{A.2}$$

$$f_\uparrow(E) = f_\downarrow(E - \delta\mu) \equiv f(E). \tag{A.3}$$

Substituting the above results into equation (A.1)

$$\langle S_z^h\rangle(\Delta, \mu_\uparrow - \mu_\downarrow) = \frac{1}{2n_h}\left[\int dE\,\{D(E) - D(E-\Delta)\} - \int dE\,\{f(E)D(E) - f(E+\delta\mu)D(E-\Delta)\}\right]. \tag{A.4}$$

The part

$$\int dE\,\{D(E) - D(E-\Delta)\} = \int dE D(E) - \int dE D(E-\Delta) = \int dE D(E) - \int dE' D(E')$$

by performing a change of variable on the second integration in the previous step. It, finally, leads to

$$\int dE\{D(E) - D(E-\Delta)\} = 0.$$

Substituting the above result in equation (A.4) we get

$$\langle S_z^h\rangle(\Delta, \mu_\uparrow - \mu_\downarrow) = \frac{1}{2n_h}\int dE\,\{f(E)D(E) - f(E+\delta\mu)D(E-\Delta)\}. \tag{A.5}$$

Proceeding further,

$$\langle S_z^h\rangle(\Delta, \mu_\uparrow - \mu_\downarrow) = \frac{1}{2n_h}\left\{\int dE\, f(E)D(E) - \int dE\, f(E+\delta\mu)D(E-\Delta)\right\} = \frac{1}{2n_h}\left\{\int dE\, f(E)D(E) - \int dE'\, f(E')D(E'-\Delta-\delta\mu)\right\}$$

by performing a change of variable on the second integration in the previous step. Finally, it leads to

$$\langle S_z^h\rangle(\Delta, \mu_\uparrow - \mu_\downarrow) = \frac{1}{2n_h}\int\{dE\, f(E)D(E) - f(E)D(E-\Delta-\delta\mu)\} \tag{A.6}$$

while substituting $\mu_\uparrow - \mu_\downarrow \equiv \delta\mu = 0$ and $\Delta = \Delta' + \delta\mu$ in equation (A.5) we find

$$\langle S_z^h\rangle(\Delta' + \delta\mu, 0) = \frac{1}{2n_h}\int dE\,\{f(E)D(E) - f(E)D(E-\Delta'-\delta\mu)\} \tag{A.7}$$

which, trivially, leads to

$$\langle S_z^h\rangle(\Delta + \mu_\uparrow - \mu_\downarrow, 0) = \frac{1}{2n_h}\int dE\,\{f(E)D(E) - f(E)D(E-\Delta-\delta\mu)\}. \tag{A.8}$$

The right-hand sides of equations (A.6) and (A.8) being equal, we equate their left-hand sides and arrive at the results in equation (9).

Appendix B. Derivation of equation (10)

Starting from equations (6) and (7), at steady state, we get

$$\frac{F_{-5/2}}{F_{-3/2}} = \frac{F_{-3/2}}{F_{-1/2}} = \cdots = \frac{F_{+3/2}}{F_{+5/2}} = \alpha \tag{B.1}$$

where we have defined

$$\alpha \equiv \frac{\Gamma_{\downarrow\uparrow}}{\Gamma_{\uparrow\downarrow}}. \tag{B.2}$$

From equation (B.1) and probability conservation: $\sum_s F_s = 1$ we get

$$\frac{F_{-5/2}}{\alpha^5} = \frac{F_{-3/2}}{\alpha^4} = \cdots = F_{+5/2} = \frac{1-\alpha}{1-\alpha^6}. \tag{B.3}$$

Substituting the above results in equation (2) we find

$$\langle S_z^{Mn}\rangle = \frac{(1-\alpha)^2}{2(1-\alpha^6)}(5\alpha^4 + 8\alpha^3 + 9\alpha^2 + 8\alpha + 5) \tag{B.4}$$

which shows that $\langle S_z^{Mn}\rangle$ *at steady state is solely a function of* α. Now, from equations (8), (A.2), (A.3) and (B.2)

$$\alpha = \frac{\int dE D(E)\{1 - f(E)\}D(E+\epsilon-\Delta)f(E+\epsilon+\delta\mu)}{\int dE D(E+\epsilon-\Delta)\{1 - f(E+\epsilon+\delta\mu)\}D(E)f(E)}. \tag{B.5}$$

For a given value of E the ratio of the integrands in the above equation

$$\frac{D(E)\{1 - f(E)\}D(E+\epsilon-\Delta)f(E+\epsilon+\delta\mu)}{D(E+\epsilon-\Delta)\{1 - f(E+\epsilon+\delta\mu)\}D(E)f(E)} = \left\{\frac{1-f(E)}{f(E)}\right\}\left\{\frac{1-f(E+\epsilon+\delta\mu)}{f(E+\epsilon+\delta\mu)}\right\}^{-1} = \exp\left\{-\frac{\epsilon+\delta\mu}{k_B T}\right\}.$$

Using the above result while treating the integrations in equation (B.5) as summation over energy and making use of the identity

$$\frac{N_1}{D_1} = \frac{N_2}{D_2} = \cdots = \frac{N_i}{D_i} = \cdots = \frac{\sum_i N_i}{\sum_i D_i}$$

we finally get

$$\alpha(\epsilon, \mu_\uparrow - \mu_\downarrow) = \exp\left\{-\frac{\epsilon + \mu_\uparrow - \mu_\downarrow}{k_B T}\right\}.$$

From the above relation it trivially follows that

$$\alpha(\epsilon, \mu_\uparrow - \mu_\downarrow) = \alpha(\epsilon + \mu_\uparrow - \mu_\downarrow, 0). \tag{B.6}$$

From the above relation and the relation in equation (B.4) (which shows that $\langle S_z^{Mn}\rangle$ at steady state is solely a function of α) we arrive at the result in equation (10).

References

[1] Wolf S A, Awschalom D D, Buhrman R A, Daughton J M, von Molnar S, Roukes M L, Chtchelkanova A Y and Treger D M 2001 *Science* **294** 1488

[2] Prinz G A 1998 *Science* **282** 1660
[3] Ohno H, Chiba D, Matsukura F, Omiya T, Abe E, Dietl T, Ohno Y and Ohtani K 2000 *Nature* **408** 944
[4] Boukari H, Kossacki P, Bertolini M, Ferrand D, Cibert J, Tatarenko S, Wasiela A, Gaj J A and Dietl T 2002 *Phys. Rev. Lett.* **88** 207204
[5] Park Y D, Hanbicki A T, Erwin S C, Hellberg C S, Sullivan J M, Mattson J E, Ambrose T F, Wilson A, Spanos G and Jonker B T 2002 *Science* **295** 651
[6] Chiba D, Yamanouchi M, Matsukura F and Ohno H 2003 *Science* **301** 943
[7] Nazmul A M, Kobayashi S, Sugahara S and Tanaka M 2004 *Japan. J. Appl. Phys.* **43** L233
[8] Chiba D, Matsukura F and Ohno H 2006 *Appl. Phys. Lett.* **89** 162505
[9] Stolichnov I, Riester S W E, Trodahl H J, Setter N, Rushforth A W, Edmonds K W, Campion R P, Foxon C T, Gallagher B L and Jungwirth T 2008 *Nat. Mater.* **7** 464
[10] Nikonov D E and Bourianoff G I 2005 *IEEE Trans. Nano.* **4** 206
[11] Ganguly S, Register L F, MacDonald A H and Banerjee S K 2006 *IEEE Trans. Nanotechnol.* **5** 30
[12] Oiwa A, Mitsumori Y, Moriya R, Słupinski T and Munekata H 2002 *Phys. Rev. Lett.* **88** 137202
[13] See for example Abragram A 1983 *Principles of Nuclear Magnetism* (New York: Oxford Uiversity Press)
Slichter C P 1990 *Principles of Magnetic Resonance* (Berlin: Springer)
[14] Wang J, Sun C, Kono J, Oiwa A, Munekata H, Cywiński Ł and Sham L J 2005 *Phys. Rev. Lett.* **95** 167401
Wang J, Cywiński Ł, Sun C, Kono J, Munekata H and Sham L J 2008 *Phys. Rev.* B **77** 235308
[15] Feher G 1959 *Phys. Rev. Lett.* **3** 135
[16] Clark W G and Feher G 1963 *Phys. Rev. Lett.* **10** 134
[17] Suhl H 2002 arXiv:cond-mat/0206215v1
[18] See for example Fert A, George J-M, Jaffres H and Mattana R 2007 *IEEE Trans. Electron. Dev.* **54** 921
Schmidt G 2005 *J. Phys. D: Appl. Phys.* **38** R107 and the references therein
[19] Saha D, Siddiqui L, Bhattacharya P, Datta S, Basu D and Holub M 2008 *Phys. Rev. Lett.* **100** 196603
[20] Siddiqui L, Saha D, Datta S and Bhattacharya P 2008 arXiv:0811.0204v1
[21] Dietl T, Haury A and Merle d'Aubigné Y 1997 *Phys. Rev.* B **55** R3347
[22] Jungwirth T, Atkinson W A, Lee B H and MacDonald A H 1999 *Phys. Rev.* B **59** 9818
[23] Dietl T, Ohno H, Matsukura F, Cibert J and Ferrand D 2000 *Science* **287** 1019
[24] Dietl T, Ohno H and Matsukura F 2001 *Phys. Rev.* B **63** 195205
[25] Jungwirth T, König J, Sinova J, Kučera J and MacDonald A H 2002 *Phys. Rev.* B **66** 012402
[26] Das Sarma S, Hwang E H and Kaminski A 2003 *Phys. Rev.* B **67** 155201
[27] Priour D J Jr, Hwang E H and Das Sarma S 2004 *Phys. Rev. Lett.* **92** 117201
[28] Ohno H, Shen A, Matsukura F, Oiwa A, Endo A, Katsumoto S and Iye Y 1996 *Appl. Phys. Lett.* **69** 363
[29] Potashnik S J, Ku K C, Chun S H, Berry J J, Samarth N and Schiffer P 2001 *Appl. Phys. Lett.* **79** 1495
[30] Cywiński Ł and Sham L J 2007 *Phys. Rev.* B **76** 045205
[31] Lipińska A, Simserides C, Trohidou K N, Goryca M, Kossaci P, Majhofer A and Dietl T 2009 *Phys. Rev.* B **79** 235322
[32] Kainz J, Schneider P, Ganichev S D, Rossler U, Wegscheider W, Weiss D, Prettl W, Belkov V V, Golub L E and Schuh D 2004 *Physica* E **22** 418
[33] Koo H C, Yi H, Ko J-B, Chang J and Han S-H 2007 *Appl. Phys. Lett.* **90** 022101
[34] Tishin A M and Spichkin Y I 2003 *The Magnetocaloric Effect and its Application* (Bristol: Institute of Physics Publishing)